Energy Conversion and Management 97 (2015) 458–469

Contents lists available at ScienceDirect

Energy Conversion and Management

journal homepage: www.elsevier.com/locate/enconman

Numerical study of cullet glass subjected to microwave heating and SiC susceptor effects. Part II: Exergy transfer analysis

Luis Acevedo, Sergio Usón *, Javier Uche

Research Centre for Energy Resources and Consumption (CIRCE), Universidad de Zaragoza, Zaragoza, Spain

ARTICLE INFO

Article history:
Received 5 December 2014
Accepted 17 March 2015
Available online 7 April 2015

Keywords:
Microwave heating
Poynting vector
Cullet glass
Susceptor
Exergy transfer

ABSTRACT

The mathematical model of exergy transfer in cullet glass heated by microwave inside of a cubical cavity with the aid of a susceptor is presented. Part I of this paper presented a numerical combined electromagnetic and heat transfer model by applying both transient Maxwell's equations and heat transfer equations. Then, the electromagnetic and temperature fields were used to obtain the exergy transfer analysis in the oven. Exergy transfer analysis informs us about the efficiency of energy transformations taking place during the heating process, since it explains how the quality of the energy behaves along the heating process. The rate of internal exergy, exergy flowing and destroyed exergy were obtained and presented for this transient process. Part I showed that the susceptor location could change the temperature fields of cullet glass. So, an exergy analysis is important to understand the irreversibilities produced by a susceptor during preheating (microwaves activation) and heating process of the cullet glass, and how they could be minimized. Exergy transfer analysis shows how both, electromagnetic and heat transfer, are responsible of the irreversibilities generated in the heating process.

1. Introduction

Exergy analysis has been developed for assessment and optimization of the efficiency of energy systems. It provides information about the efficiency of energy consumption and a better rational use of natural resources [1]. The exergy of a system represents the quantity of its energy potential when the system is not in equilibrium with the environment. Its analysis allows studying in detailed quantitative and qualitative terms, the energy transformations inside of the defined system [2–4].

Usually, exergy analysis is neglected or underutilized in other areas than thermal, mechanical or chemical systems [5]. However, in literature some examples of the exergy approach on new heating modes can be found. Petela analyzed thermal radiation process [6] and plasma systems by applying the exergy definition [7]. Saloux et al. [8] employed an exergy-electrical analogy for modeling building integrated energy systems including electric heaters, solar collectors and heat pumps. Rosen and Bulucea [9] demonstrated the usefulness of exergy in the analysis of electrical systems, particularly the electromagnet. They also showed [5] that exergy can be applied to electric devices in the same way as to thermal systems, and presented a list of electric devices with its energy and exergy efficiency analysis. The global exergy performance of a microwave furnace was analyzed by Ranjbaran and Zare in [10]. They studied the exergy analysis of a fluidized drying bed, and found the irreversibilities produced by the conversion of electromagnetic energy into heat transfer inside of the system. Formal description of the microwave heating exergy was already presented in [11], where electric and thermal concepts were appropriately linked. First, the useful energy of microwaves was defined by the Poynting vector. Then, the interactions with the environment were tackled, and finally, electric and thermal concepts were unified by describing the exergy of microwave heating.

Exergy analysis has been usually applied to steady state situations. However, it can also be very useful to analyze in detail the exergy transformations taking place in a system by quantifying the space and time dependence of exergy transfer. As stated in [12], the transition from exergy to exergy transfer is then expected as natural as the transition from heat to heat transfer. Exergy transfer studies the changes in time of the exergy value of each point in any process of a system. First attempt to define the exergy transfer process can be found in [13], where exergy transfer equation was described in 1-D. Based on this equation, Chun-Zhen et al. [14] presented a description of exergy transfer in a two dimensional thermal conduction problem. In [11] exergy transfer analysis methodology was presented and applied

* Corresponding author at: Circe Building, 15, Mariano Esquillor Gómez St, 50018 Zaragoza, Spain. Tel.: +34 976 76 1863/2956; fax: +34 976 73 2078.
E-mail addresses: leag@unizar.es, enrrique1@gmail.com (L. Acevedo), suson@unizar.es (S. Usón), javiuche@unizar.es (J. Uche).

http://dx.doi.org/10.1016/j.enconman.2015.03.065
0196-8904/

Nomenclature

A_{area}	area, m^2
a	specific exergy, J/kg
A	exergy, J
b	exergy flux, W/m^2
b'	directional exergy radiation intensity, W/sr m^2
$\dot{B}'''$	exergy flow per volume, W/m^3
$\dot{B}$	exergy flow, W
B	magnetic induction, N s/C m
Cp	specific heat, J/kg K
E	electric field intensity, V/m
E	electric field, V/m
H	magnetic field intensity, A/m
H	magnetic field, A/m
k	thermal conductivity, W/m K
$\dot{Q}'''$	heat flow per volume, W/m^3
T	temperature, °C
t	time, s
V	volume element, m^3
X	coordinate axis, m
Y	coordinate axis, m
Z	coordinate axis, m

Greek symbols

ε	permittivity, F/m
ε'	emissivity, –
μ	permeability, H/m
ρ	density, kg/m^3
σ_e	electric conductivity, S/m
σ_{SB}	Stefan–Boltzmann constant, $W/m^2\ K^4$

Subscripts

0	reference state
cond	conduction
D	destroyed
GR	gray body radiation
i	space step
j	space step
k	space step
mw	microwave

Superscripts

n	timestep

to a simple example: microwave heating of a potato layer was modeled by a finite difference scheme based on Lambert's law; in the paper the space distribution of exergy flows, exergy variation and irreversibilities involved during the microwave heating in a two dimensional process was described. In [15], exergy transfer analysis was applied to the example of a holding furnace.

This research presents the (unsteady) exergy transfer analysis of cullet glass heated by a microwave system, which is recently increasing its applicability in the industry. Here, the exergy transfer method is applied to the complex and validated model (see Part I) that contains electromagnetic and temperature fields in a 3-D cullet glass heating. As a result, the complete analysis of exergy transfer in transient state is obtained. It includes: microwave exergy, exergy transfer by conduction and radiation, accumulation of exergy and destroyed exergy (irreversibility analysis). This allows one to fully understand why the susceptor provides better results in different locations, as well as to find out irreversibilities and how exergy is transferred through cullet glass.

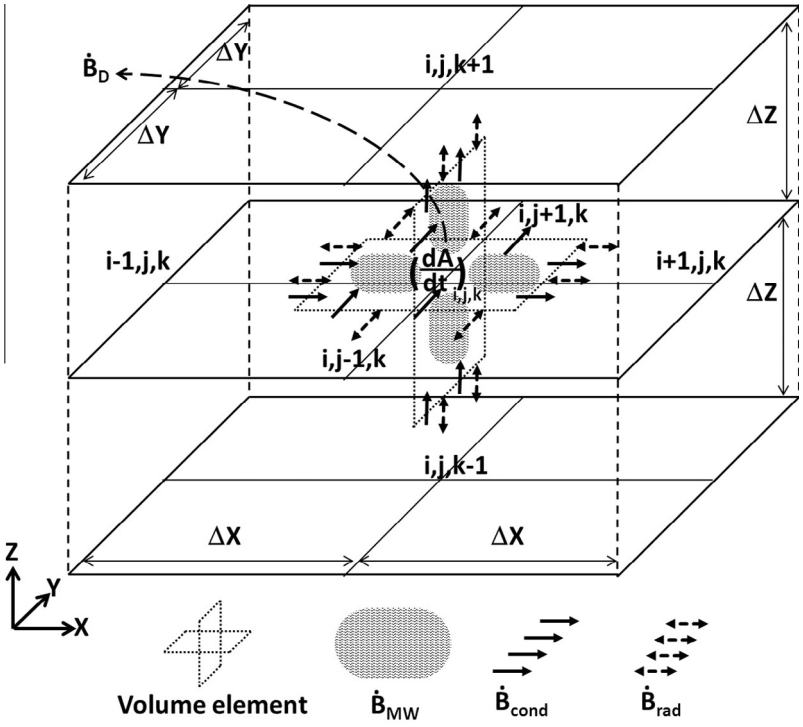

Fig. 1. Exergy transfer, general balance for a generic cell.

To sum up, exergy transfer analysis is very useful to show in detail the energy transformations happening in a system, taking into account the quantity and quality of their conversions as well as to show which are the real potential savings in those complex heating systems. This method is complementary to the temperature distribution studied in Part I; while temperature analysis shows how the heat is distributed inside of the glass, exergy transfer analysis studies the efficiency of energy transformation process.

To perform a complete exergy analysis in transient state, it is necessary to know accurate data of the temperatures and microwave energy fields in space and time. Those data were taken from Part I, where an electromagnetic and thermal model was developed and validated.

2. Exergy of microwave systems

2.1. Exergy of microwaves during heating process

In order to describe the exergy transfer inside of a microwaved working piece, first the exergy description of an electromagnetic field during heating process must be analyzed.

Poynting discovered in 1884 that electromagnetic waves carry with them electromagnetic power, and energy can be transported through the space to a distant point by these waves [16,17]. Poynting theorem represents the principle of energy conservation of electromagnetic fields, characterized by its integral form as:

$$\oint_S (\mathbf{E} \times \mathbf{H}) \cdot ds = -\frac{\partial}{\partial t} \int_V \left(\frac{1}{2} \varepsilon E^2 + \frac{1}{2} \mu H^2 \right) dV - \int_V \sigma_e E^2 dV \qquad (1)$$

Left side of Eq. (1) is the electromagnetic energy leaving an enclosed surface (given by the Poynting vector). First term in the right side of Eq. (1) is the time-rate of reduction of energy stored in the electric field. Second term is the time-rate of reduction of energy stored in the magnetic field, and the last term is the ohmic power dissipated in the volume due to the flow of current density $\sigma\mathbf{E}$ in the presence of the electric field $\mathbf{E}$.

If an ideal suitable device is defined, the maximum work produced while interacting only with the environment can be obtained [6]. This approach was applied in [11], where it is shown that the equation containing the exergy of a microwave is the Poynting vector:

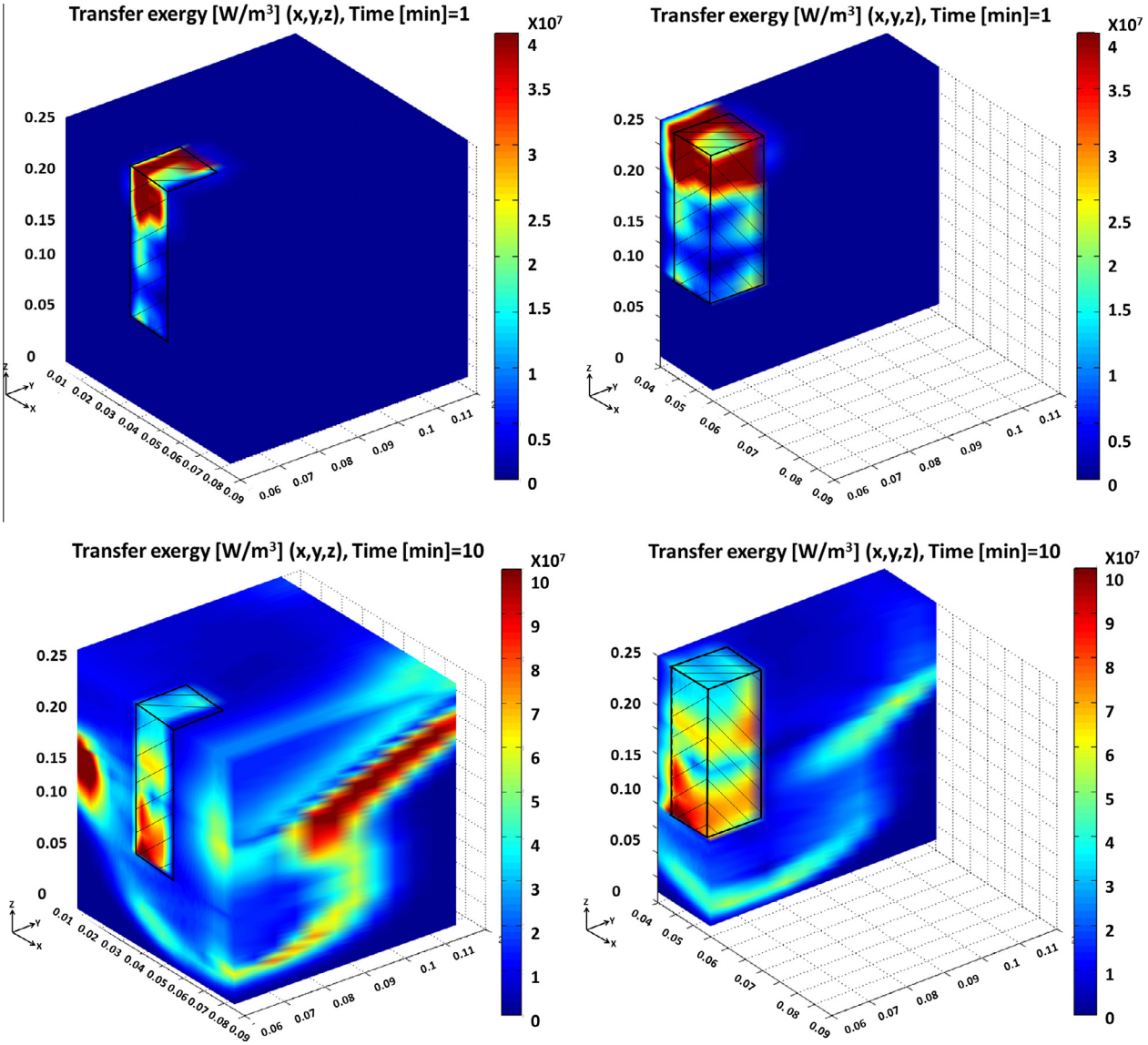

Fig. 2. Transfer exergy by conduction and radiation at minutes 1 and 10.

$$\dot{B}_{MW} = \int (\mathbf{E} \times \mathbf{H}) \cdot dS \tag{2}$$

This means that Poynting vector also represents exergy of electromagnetic waves; thus, during a microwave heating process, exergy provided by microwaves is equal (in magnitude) to the energy.

2.2. General exergy transfer model

The differential equation of exergy transfer process was previously studied in [18], where fluid movement was included, but not an input exergy source (like microwaves). The exergy equation for a solid with a constant density and thermal conductivity affected by microwaves is then:

$$\nabla \cdot \left[k \nabla T \left(1 - \frac{T_0}{T} \right) \right] + \dot{B}'''_{mw} = \rho \frac{da}{dt} + \dot{B}'''_{D} \tag{3}$$

Left side of Eq. (3) represents the exergy entering the differential volume due to thermal conduction (heat conduction flow times the Carnot factor) and the exergy transferred by microwaves $\dot{B}'''_{mw}$. On the right side, the exergy accumulation and exergy destroyed terms are found. In other words, Eq. (3) states that exergy gain, due to conduction and microwaves heating, is either accumulated or destroyed.

Electromagnetic and thermal models presented in Part I were able to compute temperature fields and energy flows of the complete system. Results obtained in Part I were verified and validated according to the same procedure followed in [19]. Solutions found for electromagnetic and thermal fields during microwave heating of mullite were used for the validation. Once temperature field is calculated and validated, exergy transfer method can be developed without the need of further validation.

To perform a more detailed analysis of energy transformations, the next step is to apply the exergy transfer model of Eq. (3).

3. Exergy transfer during microwave heating

A discretized form of Eq. (3) is the general exergy balance of a finite volume (in Watts) presented in Eq. (4).

$$\dot{B}_{(i+1,j,k)} + \dot{B}_{(i-1,j,k)} + \dot{B}_{(i,j+1,k)} + \dot{B}_{(i,j-1,k)} + \dot{B}_{(i,j,k+1)} + \dot{B}_{(i,j,k-1)} + \dot{B}_{MW} = \left(\frac{dA}{dt} \right)_{(i,j,k)} + \dot{B}_{D(i,j,k)} \tag{4}$$

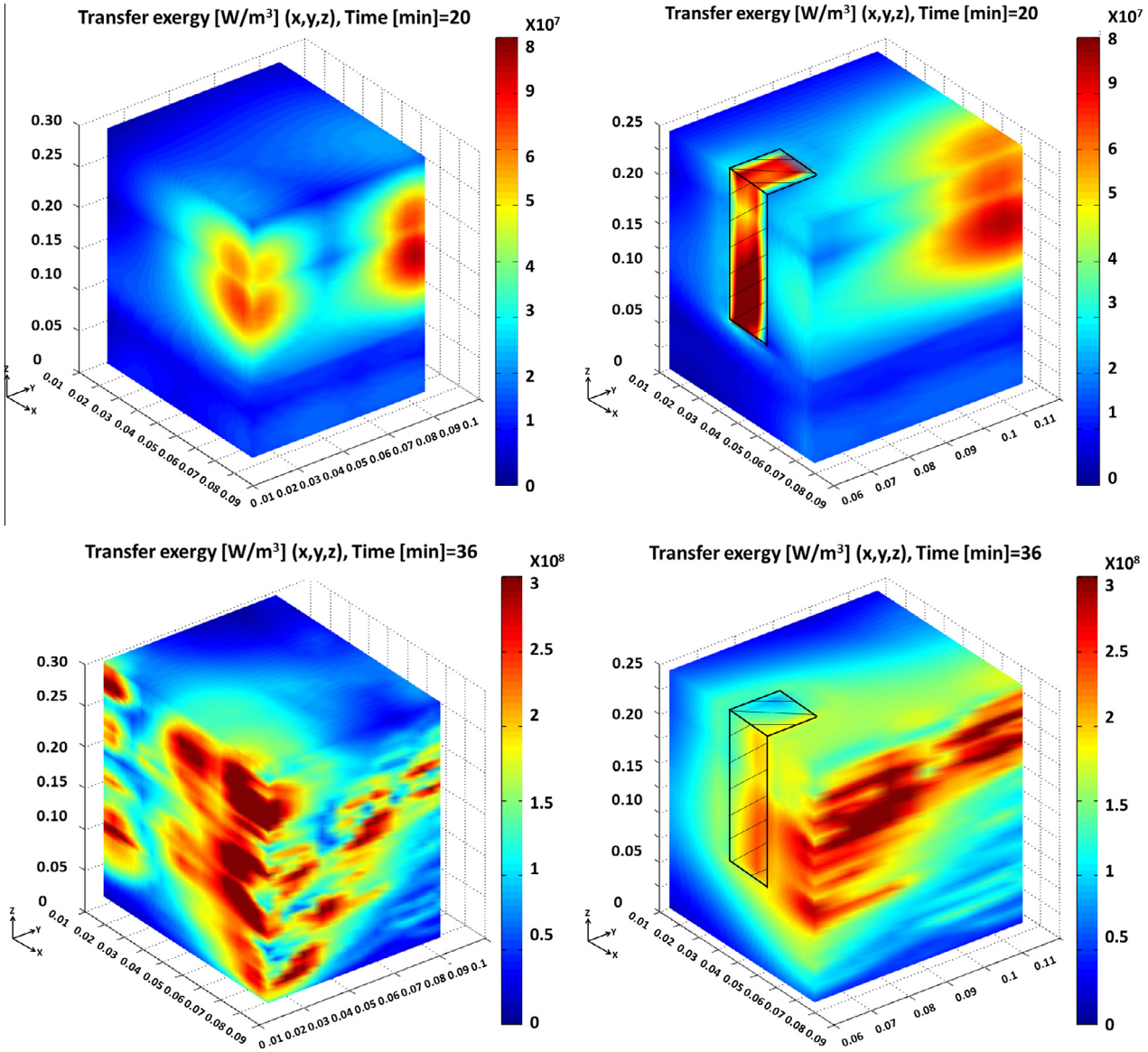

Fig. 3. Transfer exergy by conduction and radiation at minute 20 and at the end of the process (approximately 36 min).

The terms of the exergy balance presented in Eq. (4) are described as:

- $\dot{B}_{(i,j,k)}$: Exergy transferred by conduction and radiation.
- $\dot{B}_{MW}$: Exergy from microwaves.
- $dA_{(i,j,k)}$: Change of internal exergy.
- $\dot{B}_D$: Destroyed exergy.

Fig. 1 shows a graphic definition of these terms. Its evaluation is discussed below.

Three forms of exergy transfer were considered in the analysis: Microwave input provoked by the electromagnetic field, conduction inside of the cullet glass, and radiation exchange between susceptor and cullet glass.

3.1. Three-dimensional microwave exergy input

As demonstrated in [11], exergy of microwaves is equal to its energy. This means that exergy of the electromagnetic field coincide in magnitude with the heat generated in the cullet glass due to microwave action. Then, microwave heating exergy is equal to the volumetric generation inside of the glass, as presented in Part I:

$$\dot{B}_{MW(i,j,k)} = \Delta x \Delta y \Delta z \dot{Q}'''_{MW(i,j,k)} \tag{5}$$

In the center of the cell, the change in the non-flow exergy term A was evaluated based on the temperature changes produced by heat transfer:

$$\frac{dA_{(i,j,k)}}{dt} \cong \frac{\Delta z \cdot \Delta x \cdot \Delta y \cdot \rho \cdot C_p \left[\left(T^n_{(i,j,k)} - T^{n-1}_{(i,j,k)} \right) + T_0 \ln \left(\frac{T^{n-1}_{(i,j,k)}}{T^n_{(i,j,k)}} \right) \right]}{\Delta t} \tag{6}$$

In which T_0 is the environment absolute temperature.

Finally, the first six terms of the left hand side of Eq. (4) represent the exergy transfer by conduction (for an inner cell) and radiation (for cells located at susceptor boundary). These terms are explained in the next section.

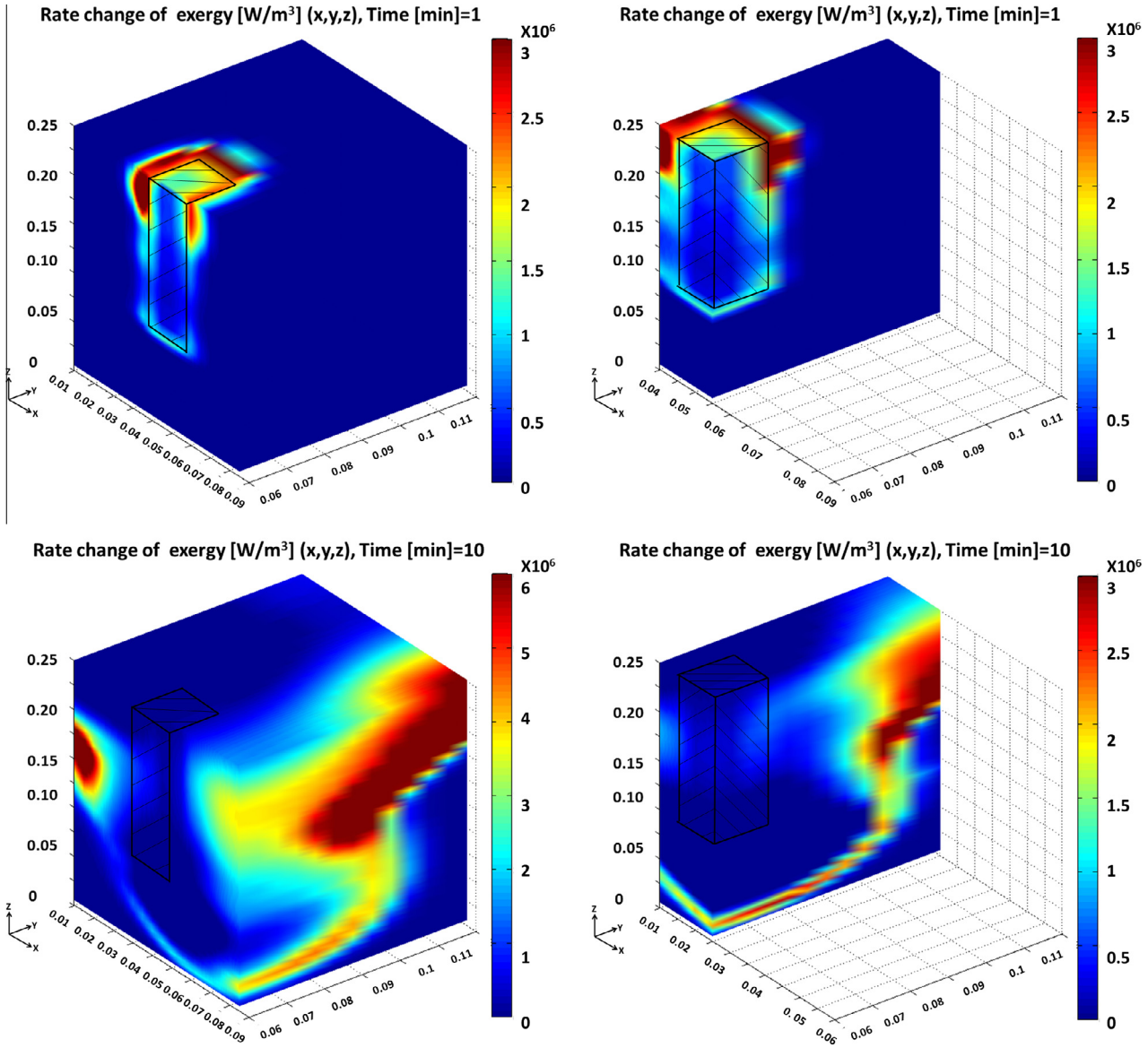

Fig. 4. Rate change of exergy at minutes 1 and 10 respectively.

3.2. Three-dimensional exergy transfer in inner nodes

Exergy of conduction was computed by using the Carnot factor. For that reason, the evaluation of first six terms of Eq. (4) depends on the specific condition of the boundaries. It was assumed that temperature at the boundary was the average temperature between the nodes. According to Fig. 1, exergy exchanged by conduction in i direction with node $(i+1,j,k)$ was:

$$\dot{B}_{cond(i+1,j,k)} = \Delta y \cdot \Delta z \cdot k\left(\frac{T_{(i,j,k)} - T_{(i+1,j,k)}}{\Delta x}\right)\left(1 - \frac{2T_0}{T_{(i,j,k)} + T_{(i+1,j,k)}}\right) \quad (7)$$

Similarly, for nodes in j and k directions:

$$\dot{B}_{cond(i,j+1,k)} = \Delta x \cdot \Delta z \cdot k\left(\frac{T_{(i,j,k)} - T_{(i,j+1,k)}}{\Delta y}\right)\left(1 - \frac{2T_0}{T_{(i,j,k)} + T_{(i,j+1,k)}}\right) \quad (8)$$

$$\dot{B}_{cond(i,j,k+1)} = \Delta x \cdot \Delta y \cdot k\left(\frac{T_{(i,j,k)} - T_{(i,j,k+1)}}{\Delta z}\right)\left(1 - \frac{2T_0}{T_{(i,j,k)} + T_{(i,j,k+1)}}\right) \quad (9)$$

As explained in Part I, in Eqs. (7)–(9), thermal conductivity k includes the internal radiation term by means of the effective conductivity k_{eff}.

3.3. Exergy transfer in susceptor boundary nodes

When the node is in the boundary between glass and susceptor, radiation effects have also to be considered. Part I demonstrated that it was the main heat transfer mode between the susceptor and the glass.

Exergy loss due to radiation emission, absorption and scattering processes is consistent with the Gouy–Stodola theorem [20]. For the particular case of exergy flux and exergy destruction during a radiation process, Liu and Chu [21] proposed the equation of the net local rate of exergy gained by a wall medium under the

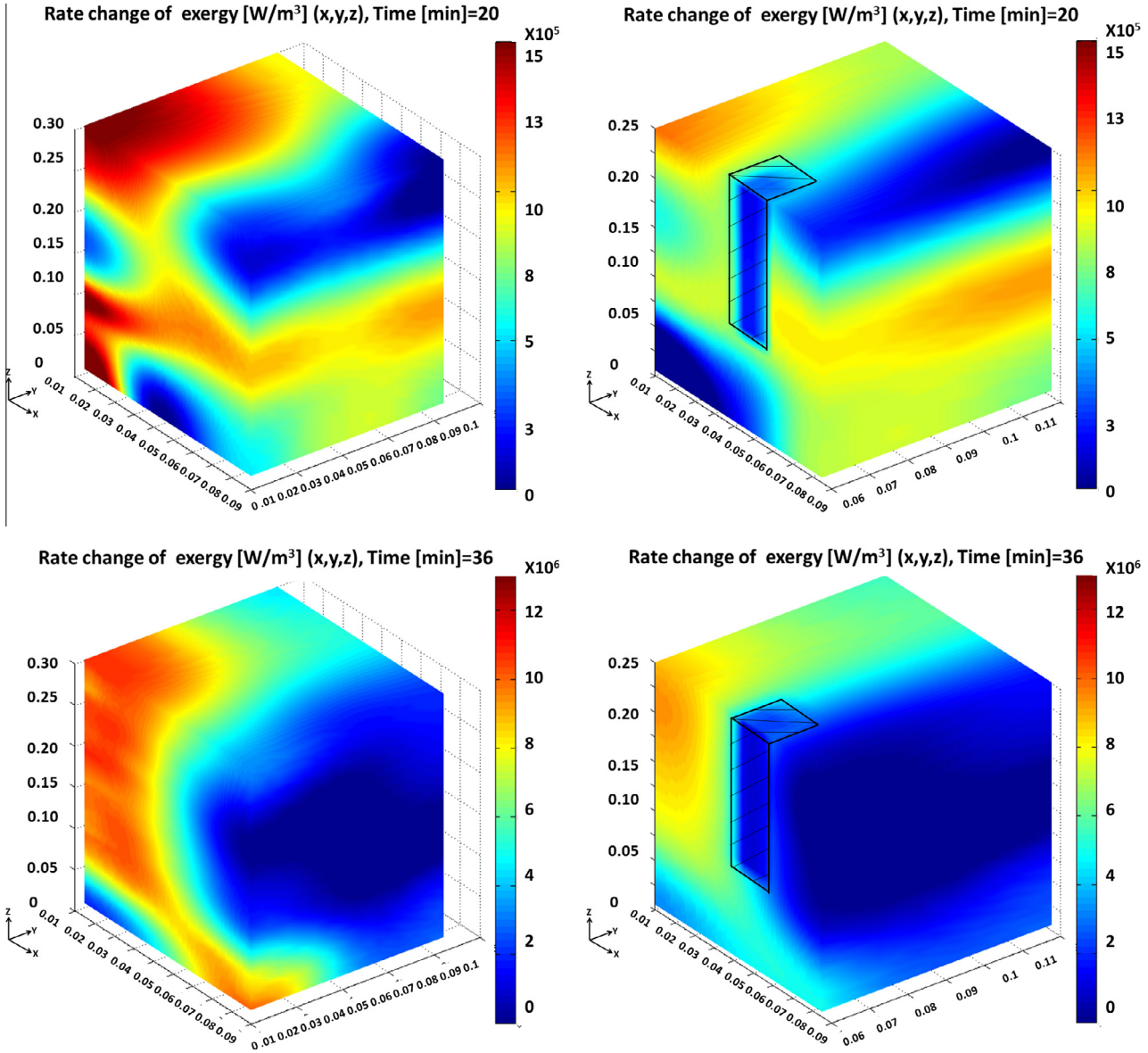

Fig. 5. Rate change of exergy at minute 20 and at the end of the process (approximately 36 min).

radiative influence. However, to date no quantitative studies about exergy transfer of radiation have been found in literature. A good approximation to the real exergy transfer by means of radiation could be made by computing the directional exergy radiation intensity for a diffuse gray body radiation. As explained in [22], using the directional entropy radiation intensity of a diffuse gray body, and integrating over the whole wavelength spectrum, it was found that:

$$b'_{GR} = \frac{\sigma_{SB}}{\pi} T^4 \left\{ \begin{array}{l} \varepsilon' - \frac{4}{3}\frac{T_0}{T}\varepsilon' \left[1 - \frac{45}{4\pi^4}(2.311 - 0.175\varepsilon')\ln(\varepsilon')\right] + \\ \frac{1}{3}\left(\frac{T_0}{T}\right)^4 \end{array} \right\} \quad (10)$$

where σ_{SB} is the Stefan–Boltzmann constant, ε the emissivity, T_0 the reference temperature and T the body temperature. Exergy flux of a diffuse radiation is then:

$$b_{GR} = \pi b'_{GR} \quad (11)$$

Finally, the exergy flux provoked by the radiative exchange between susceptor and cullet glass was computed as:

$$\dot{B}_{rad} = A_{area} \cdot \sigma_{SB} T^4 \left\{ \varepsilon' - \frac{4}{3}\frac{T_0}{T}\varepsilon \left[1 - \frac{45}{4\pi^4}(2.311 - 0.175\varepsilon)\ln(\varepsilon')\right] + \frac{1}{3}\left(\frac{T_0}{T}\right)^4 \right\} \quad (12)$$

where A_{area} is the area ($\Delta x \cdot \Delta y$, $\Delta y \cdot \Delta z$ or $\Delta x \cdot \Delta z$ depending on the orientation of the surface).

The total exergy flux was then obtained by the addition of the exergy by conduction term and radiation obtained in Eq. (12):

$$\dot{B}_{tot} = \dot{B}_{cond} + \dot{B}_{rad} \quad (13)$$

4. Case study: cullet glass heating activated by SiC susceptor (base case)

In Part I of this work, a SiC susceptor was studied by means of a heat transfer and electromagnetic model. Four susceptor positions were analyzed and compared. In this section, those positions are studied through the exergy transfer analysis (Second Law

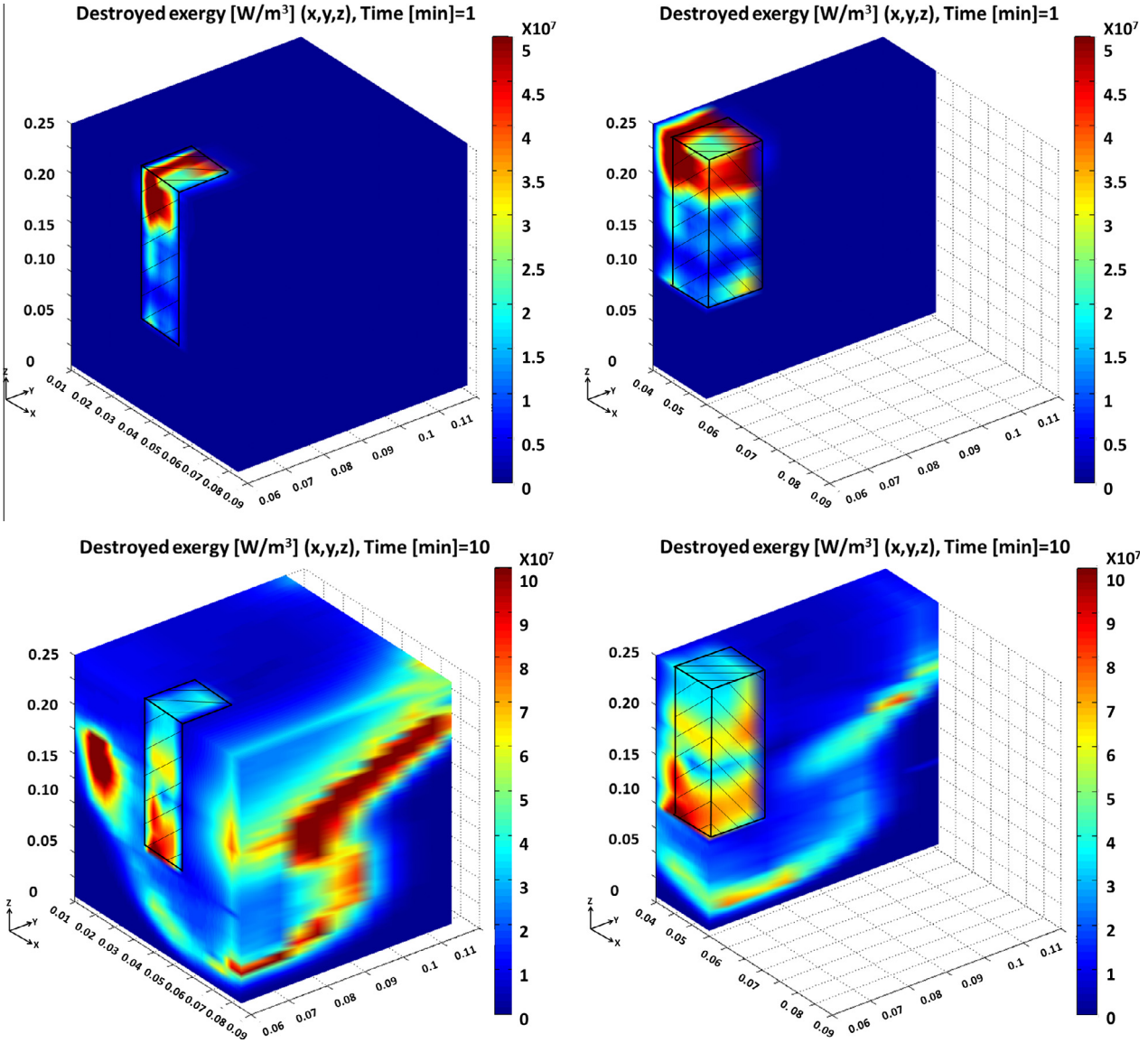

Fig. 6. Destroyed exergy at minutes 1 and 10.

perspective in transient problems). Case base (case *A*) is analyzed to fully understand the applied methodology, and then all cases (*A*–*D*) are compared.

4.1. Exergy transferred by microwave

Microwave exergy input coincides in magnitude with the microwave power (Q''_{mw}) absorbed by the cullet glass; these results can be found in Fig. 13 of Part I.

4.2. Exergy transferred by conduction and radiation

Figs. 2 and 3 represent the evolution of the exergy transferred inside of the cullet glass. After 1 min of operation, SiC susceptor absorbs and converts microwave exergy into transferrable exergy by conduction and radiation. Then, exergy is transferred from the susceptor to the cullet glass in order to activate it.

Once the glass is completely activated (minute 10), exergy transfer decreases inside of the susceptor but increases in the glass as it is becoming able to fully absorb the applied microwaves.

Hotspots found in Part I produce a high amount of exergy transfer inside of the cullet. This kind of spots, at first, generates high exergy activity. However, they also generate irreversibilities that strongly reduce the overall heating process efficiency.

After 20 min of simulation, most of the exergy transfer is concentrated on the corners and inside of the susceptor. However, at the end of the process, the exergy transfer activity found is higher in the cullet areas near to the microwave source.

4.3. Rate change of internal exergy

Due to the microwave supply into the applicator and its further effect on heat transfer by means of conduction and radiation, the temperature and thus the exergy of the cullet glass is increased along the time. In this variable (exergy rate change), the same pattern appears: susceptor initiates the process, then glass increases its exergy, and finally external walls obtain the highest amount of exergy rate changes (Figs. 4 and 5).

It is important to remember that specific thermal and dielectric properties of susceptor permit not only a better microwave

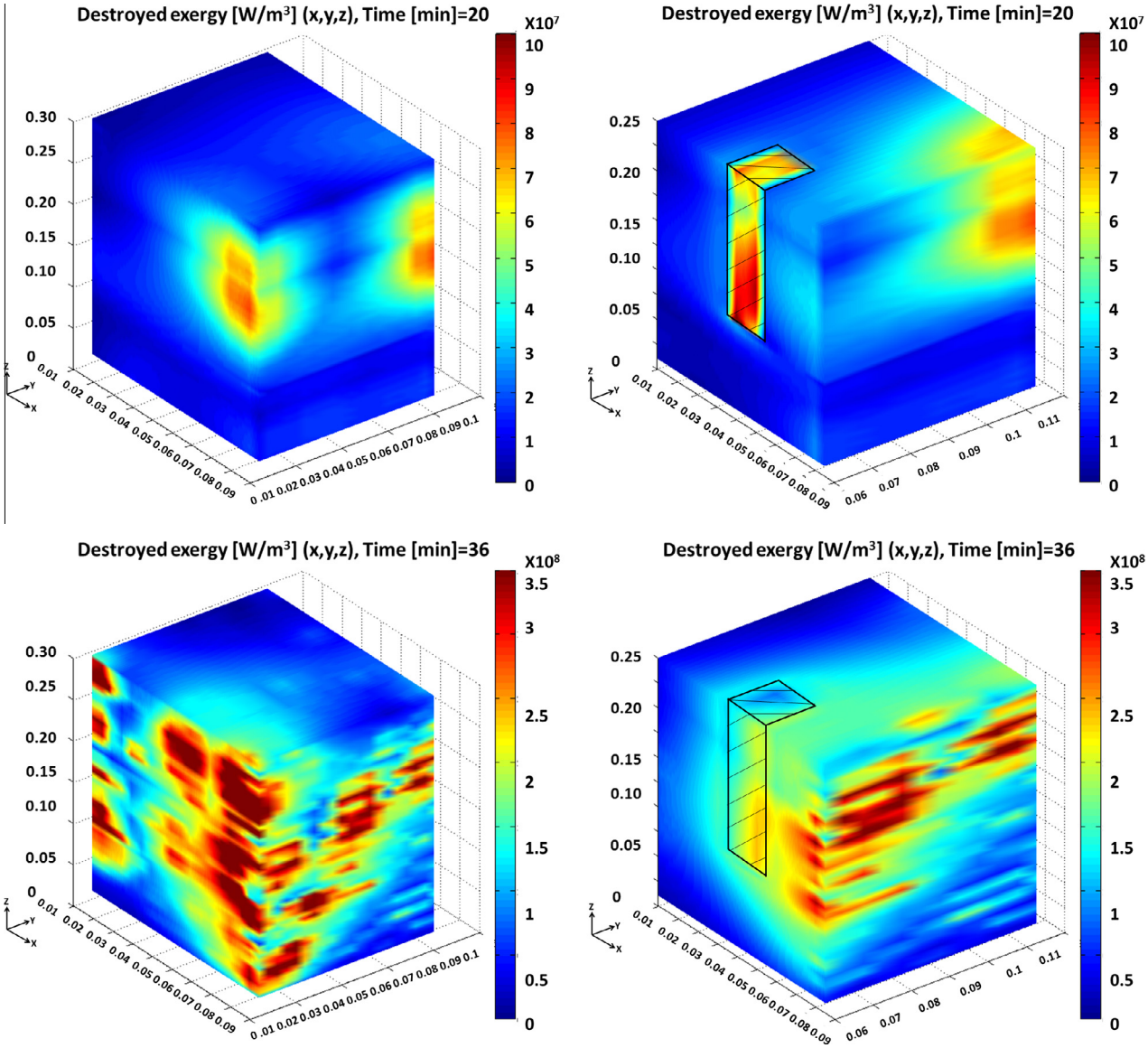

Fig. 7. Destroyed exergy at minute 20 and at the end of the process (approximately 36 min).

absorption, but also a higher amount of heat transferred to the cullet. This difference could be easily appreciated in the first minutes of the cullet activation. After 1 min of starting the simulation, susceptor increases very fast its temperature, and therefore its exergy content. However, once the cullet is activated, susceptor temperature is smoothly increased and therefore the rate change of exergy is considerably reduced, if compared with those rates found inside of the cullet glass.

Rate change of exergy can be considered as a very good indicator of the thermal stability of the process and, consequently, of its product quality. Glass melting process requires a very stable temperature and the rate change of exergy analysis permits to identify those zones where more or less exergy rate will be required to reach local thermal equilibrium. In Fig. 5, it can be observed that, after 20 min, exergy is concentrated in the corners, but in the center the equilibrium has not been completely obtained. At the end, the external wall far from the microwave source is still changing its amount of exergy rate, while in the center and in the wall next to that microwave source, thermal equilibrium has already been reached.

4.4. Destroyed exergy

Some part of the exergy provided by microwaves, and then transferred by conduction and radiation that is not accumulated is consequently destroyed. Exergy destroyed appears in Figs. 6 and 7. It can be seen how exergy destruction values are rather close to that one provided by the exergy of microwaves, which were already computed in Part I. The analysis shows that even if the transfer of exergy process is not so efficient at low temperatures, the way that exergy enters to the cullet glass permits to accelerate the target temperatures.

The exergy delivered from microwaves to the cullet glass produces a high amount of irreversibilities but they are increased in a lower rate than the internal exergy of the product. Therefore, the temperature is also increased faster than in conventional ovens.

Anyway, this analysis shows that the main source of exergy destruction is the application of high quality energy (microwaves) and not the susceptor presence. Figs. 6 and 7 completely agreed with those presented for the transfer and rate changes of exergy: at the beginning of the heating process, only SiC produces the

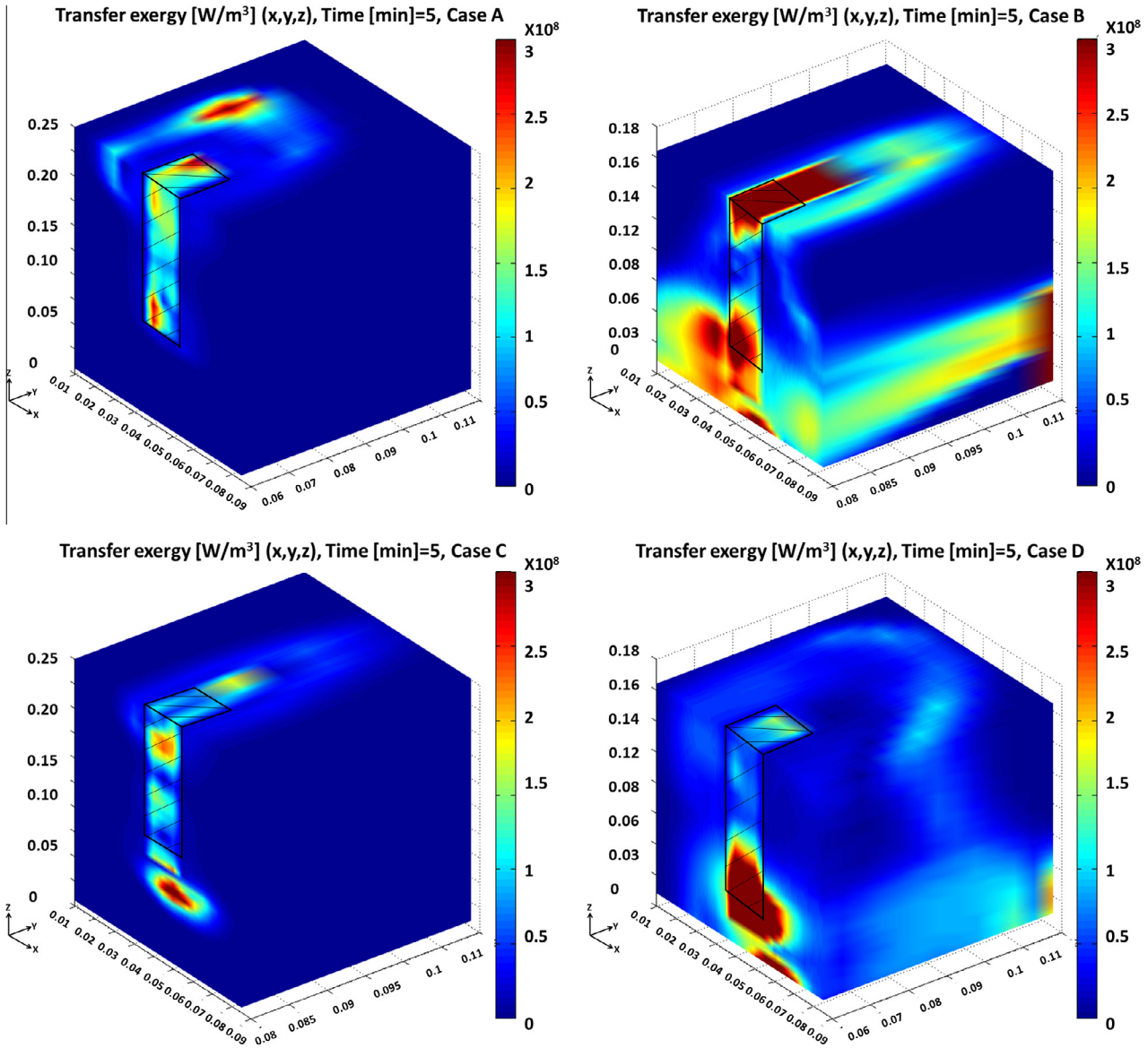

Fig. 8. Exergy transfer by conduction and radiation in all SiC positions.

exergy activity, and in the end the activity it is focused on the external walls of the applicator, especially that one close to the microwave source.

5. Analysis of the effect of SiC susceptor position based on exergy transfer analysis

As explained in Part I of this paper, when the material inside of the applicator varies its location, the effects on electromagnetic fields present important variations, thereby producing different heating patterns.

Exergy transfer of the SiC susceptor at different positions shows important variations in the irreversibilities found. Susceptor positions presented in Part I were maintained. The simulations presented here show 5 min of activity (see Fig. 8), when susceptor is fully activated by microwave heating.

5.1. Exergy transfer by conduction and radiation

Fig. 8 shows how exergy transferred by conduction and radiation coming from the susceptor in cases *B* and *D* produces more active interactions between the SiC and cullet glass. In cases *A* and C, only a few high exergy transfer spots are produced in the top and the bottom of the susceptor, respectively. Thus, it seems that locations *B* and *D* could be more efficient place for the susceptor to perform the cullet glass heating process, as it is suggested in Part I.

5.2. Rate change of exergy

In order to check thermal stability of the process, the cases with more hotspots could be identified by comparing the SiC positions during the activation of the cullet glass heating process.

Fig. 9 presents how the highest rate change of exergy in cullet appears in case *D*. After 5 min of applying microwaves, this case presents more exergy activity (exergy rate change) inside of the cullet glass than the others. Case *B* also presents a reasonable exergy activity, but it is only found at the bottom of the applicator. In cases *A* and *C*, the activity inside of the cullet glass is relatively low and concentrated on local hotspots.

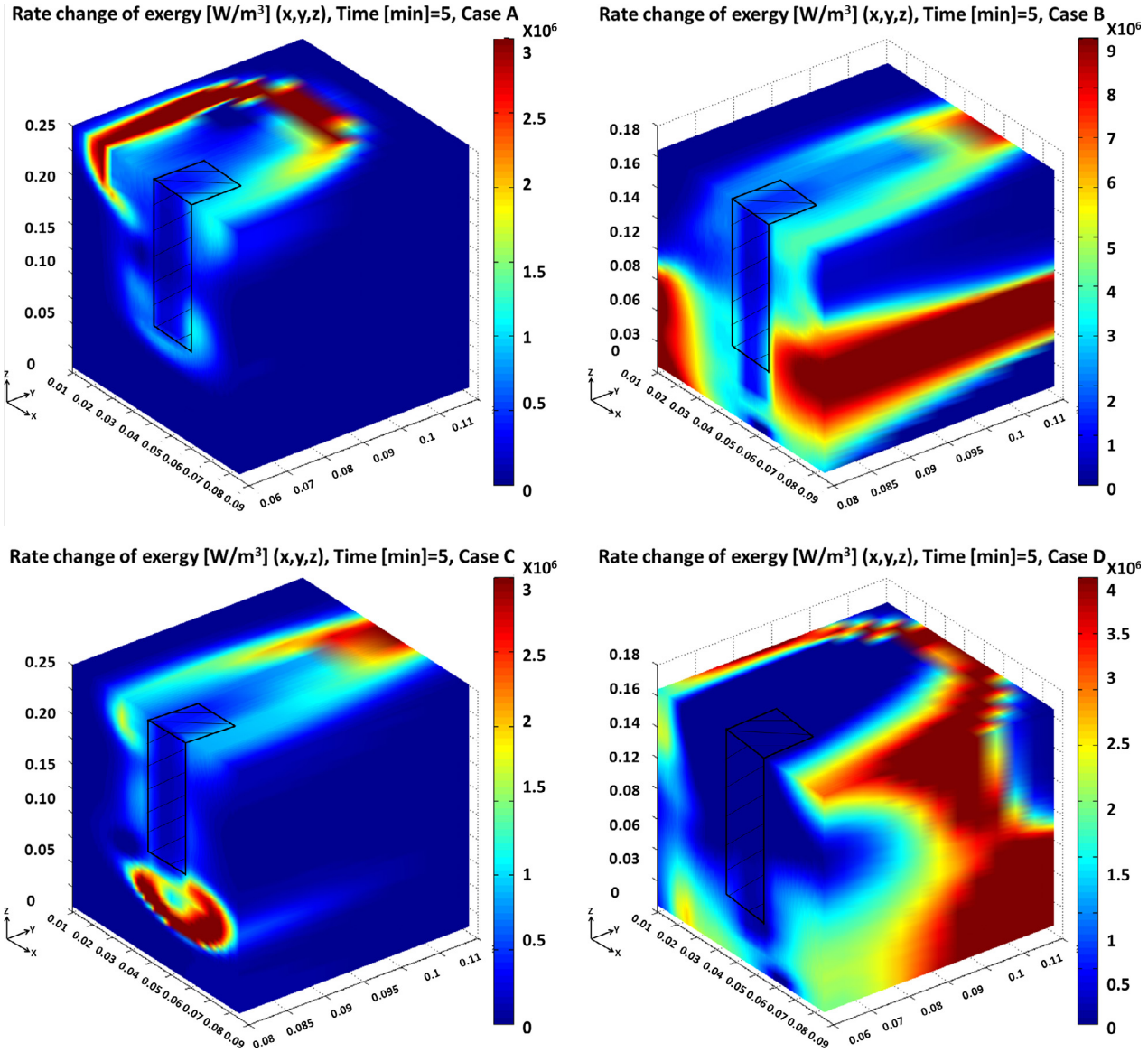

Fig. 9. Rate change of exergy at different SiC positions.

5.3. Destroyed exergy

Exergy destruction indicates the amount of irreversibilities produced during the heating process. Thus, it points out whether there exist or not any potential for the improvement of the energy efficiency of the heating process.

The destroyed exergy presented in Fig. 10 demonstrates that after 5 min case *B* concentrates the exergy destruction at the top of susceptor, whereas case *D* does the same at the bottom. For cases *A* and *C*, exergy destruction is mainly distributed along the susceptor surface. This occurs because glass activation has not been performed for those cases, what implies that more heating time is required and less energy efficiency is therefore obtained.

5.4. Global effect

In order to compare the four susceptor locations, it is also interesting to calculate aggregated values of exergy; in other words, to perform the overall exergy balances inside of the cullet glass furnace heated by the microwave source. These global exergy balances appear in Table 1. In microwave heating case A, 10,899 kJ of exergy are delivered to the glass and susceptor, and only about 62.1% is accumulated in the glass (useful effect).

Table 1
Global exergy analysis.

Case	Material	Accumulated exergy (kJ)	Destroyed exergy (kJ)	Microwave exergy (kJ)	Exergy efficiency (–)
A	Glass	6750	4110	10,899	62.1%
	Susceptor	19.30	11.77		
	Total	6769.3	4121.77		
B	Glass	6740	3760	10,533	64.2%
	Susceptor	17.19	9.58		
	Total	6757.19	3769.58		
C	Glass	6730	3940	10,746	63.2%
	Susceptor	18.53	10.79		
	Total	6748.53	3950.79		
D	Glass	6740	3970	10,749	62.9%
	Susceptor	17.26	10.16		
	Total	6757.26	3980.16		

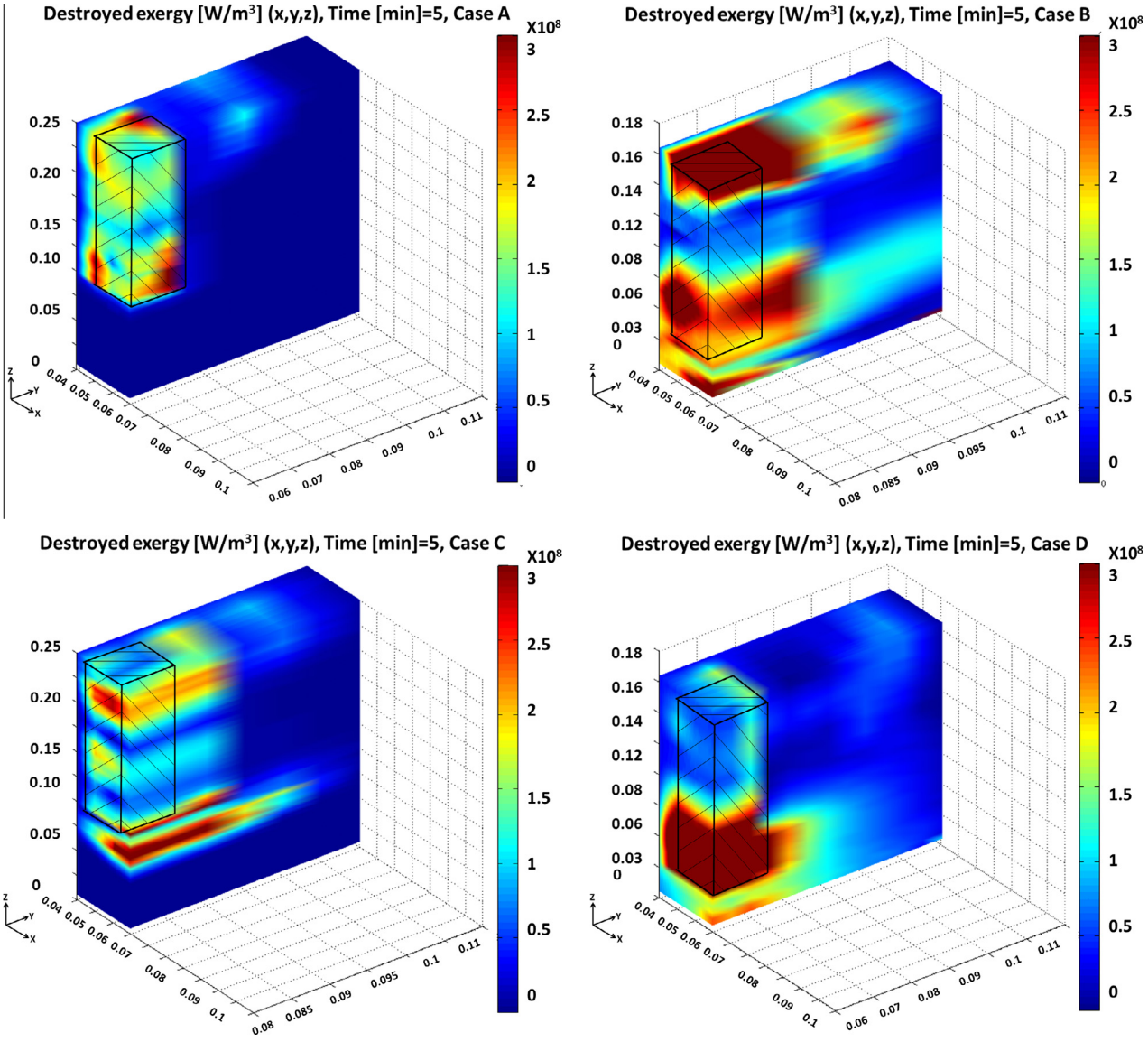

Fig. 10. Total destroyed exergy at different SiC positions.

Although in case *A*, the highest exergy accumulation term for susceptor and glass is found, this case is the less efficient due to the high amount of irreversibilities generated (destroyed exergy). Similar results are found in case *D*. On the other hand, case *C* produces less irreversibilities than any other case, nevertheless the accumulation term is also small and the efficiency found is not the best. Finally, at the end, in case *B* less exergy is needed for achieving the target temperature point. It should be noted that the heating process is finished when the whole cullet glass reached an average temperature of 1300 C. For this reason, and due to hotspots, there are small differences in the accumulated exergy.

6. Conclusions

Exergy transfer analysis was proposed here for a detailed analysis of the efficiency of cullet glass heating under the effects of an electromagnetic field produced by microwaves. It should be noted that this method is complementary to the temperature distribution and to the global efficiency analysis, and could be also applied on any other complex energy system or process. Temperature analysis shows how heat is distributed inside of the cullet glass and susceptor, and exergy transfer analysis shows the evolution of the energy efficiency of the heating process, the irreversibilities (mainly produced by hotspots) and how they can be reduced by analyzing different susceptor positions. Thus, exergy transfer explains the way in which energy coming from microwaves is being transferred to the load and how it loses its quality.

A more detailed analysis including local exergy cost of microwave heating could be found in [23]. This approach analyzes in detail the amount of exergy required to the product, taking into account the efficiency of the applied technologies and the energy conversion process.

The formulation of exergy transfer presented includes the supply of microwave exergy, exergy transfer by conduction and radiation, accumulation of exergy in transient periods and destroyed exergy (irreversibilities). This study demonstrates that depending on the susceptor position, the final temperature and the magnetic field distribution varies a lot and this fact could produce more or less irreversibilities during the cullet glass heating.

In Part I, the temperature analysis estimated the hotspots locations at each susceptor position. This analysis showed that case *D* produces less hotspots and allows obtaining a better quality product. However, a detailed exergy transfer process performed here permits to observe that actually case *B* is a better option due to its higher exergy efficiency. Although in case *A* less irreversibilities are produced during the cullet activation, after 30 min of operation, a higher amount of irreversibilities were found.

Finally, as shown in Figs. 8–10, case *B* initiates first the cullet glass activation: Targeted temperatures are early obtained, and therefore it has the best overall exergy and energy efficiency.

Acknowledgments

First author acknowledges the support from Mexican *Consejo Nacional de Ciencia y Tecnologia* (*CONACYT*) through the scholarship number 25712. This work has been carried out with the support of grant of the *Secretaría de Educación Pública* (*SEP*) and the Mexican Government.

References

[1] Dincer I, Cengel Y. Energy, entropy and exergy concepts and their roles in thermal engineering. Entropy 2001;3:116–49.
[2] Szargut J. Exergy method: technical and ecological applications (developments in heat transfer). WIT press; 2005.
[3] Kotas J. The exergy method of thermal plant analysis. Butterworths; 1985.
[4] Lozano M, Valero A. Theory of the exergetic cost. Energy 1993;18(9):936–60.
[5] Rosen M, Bulucea C. Using exergy to understand and improve the efficiency of electrical power technologies. Entropy 2009;11:820–35.
[6] Petela R. Exergy of undiluted thermal radiation. Sol Energy 2003;74:469–88.
[7] Petela R, Piotrowicz A. Exergy of plasma. Archiwum termodynamiki i spalania 1977;8:381–91.
[8] Saloux E, Teyssedou A, Sorin M. Development of an exergy-electrical analogy for visualizing and modeling building integrated energy systems. Energy Convers Manage 2015;89:907–18.
[9] Rosen M, Bulucea C. Assessing electrical systems via exergy: a dualist view incorporating technical and environmental dimensions. In: Proceedings of the 6th WSEAS international conference on engineering education. vol. 1; 2009. p. 116–23.
[10] Ranjbaran M, Zare D. Simulation of energetic and exergetic performance of microwave-assisted fluidized bed drying of soybeams. Energy 2013;59:484–93.
[11] Acevedo L, Usón S, Uche J. Exergy transfer analysis of microwave heating systems. Energy 2014;68:349–63.
[12] Qing-lin C, Yao X. The thermodynamic background of exergy transfer. In: Power and energy engineering conference (APPEEC). vol. 1; 2010. p. 1–4.
[13] Soma J. Exergy transfer: a new field of energy endeavor. Energy Eng 1985;82:11–22.
[14] Chun-Zhen Q, Xin-Yao X, Zhao-Yun W. Description of exergy transfer in the two dimensional thermal conduction process. J Eng Thermophys 2003;24:202–2043.
[15] Acevedo L, Usón S, Uche J. Exergy transfer analysis of an aluminum holding furnace. Energy Convers Manage 2015;89:484–96.
[16] Cheng D. Field and wave electromagnetics. 2nd ed. USA: Addison-Wesley; 1983.
[17] Poynting J. On the transfer of energy in the electromagnetic field. Philos Trans 1884;175:342–61.
[18] Rangel V, Usón S, Cortés C, Valero A. Local exergy cost theory. In: ASME international mechanical engineering congress; 2004.
[19] Vaz R, Pereira J, Ervilha A, Pereira JC. Simulation and uncertainty quantification in high temperature microwave heating. Appl Therm Eng 2014;70:1025–39.
[20] Makhanlall D, Liu L. Second law analysis of coupled conduction–radiation heat transfer with phase change. Int J Therm Sci 2010;49:1829–36.
[21] Liu L, Chu S. Radiative exergy transfer equation. J Thermophys Heat Transfer 2007;21(4):819–22.
[22] Agudelo A, Cortés C. Thermal radiation and the second law. Energy 2010;35:679–91.
[23] Acevedo L, Usón S, Uche J. Local exergy cost analysis of microwave heating systems. Energy 2015;80(437):451.